FIG. 1. Ratio of propagated NSI to SI atmospheric fluxes at detector level. We set $\epsilon_{\mu\tau} = -0.05$, and all other NSI parameters to zero. Dotted (dashed) lines show the regions in which 99% of the DeepCore (IceCube) MC events are contained. *Left panel:* Propagated fluxes of ν_e and ν_τ neutrinos and anti-neutrinos. *Right panel:* Propagated fluxes of ν_μ neutrinos and anti-neutrinos

I. METHODOLOGY

The neutrino flux at the detector is calculated by propagating the atmospheric neutrino flux [1] through the Earth by solving the Schrödinger equation for varying density. The Earth density profile is taken from the PREM [2]. The baseline for a given trajectory is determined using an average neutrino production height of 15 km and an Earth radius of 6371 km.

The oscillation probability $P_{\alpha\beta}$ acts as a weight to the atmospheric flux, yielding the propagated flux at detector level for flavor β as

$$\phi_\beta^{\text{det}} = \sum_\alpha P_{\alpha\beta} \phi_\alpha^{\text{atm}}, \tag{1}$$

where we sum over the initial lepton flavors $\alpha \in \{e, \mu, \bar{e}, \bar{\mu}\}$. To illustrate the impact of $\epsilon_{\mu\tau}$ on both probability and flux level, we plot the oscillograms resulting from Eq.1 in Fig. 1. In the left panel, we have marked the region in which 99% of the DeepCore cascade events originating from ν_e and ν_τ fluxes are contained. In the right panel, we show the two regions in which 99% of the IceCube and DeepCore track events originating from ν_μ fluxes are contained. Starting with the ν_μ flux ratio, we see that the only clear signal discernible to the IceCube detector is a flux deficiency of a factor of $\sim 10^2$ from core-crossing neutrinos within a zenith range of $\cos(\theta_z^{true}) > -0.87$. DeepCore, on the other hand, observes multiple fringes of flux surpluses with a factor $\sim 10^1$. The strongest surplus at 20 GeV is very weakly zenith dependent, a stark contrast to the energy-independent but zenith-sensetive IceCube deficiency.

For the fluxes which drives cascades, we have to resort to the DeepCore detector alone. Here we see a somewhat weaker signal, this time a zenith-independent deficiency.

A. IceCube

The event rate for each bin reads

$$N_{ij} = T \int_{(\cos\theta_z^r)_i}^{(\cos\theta_z^r)_{i+1}} \mathrm{d}\cos\theta_z^r \int_{E_j^r}^{E_{j+1}^r} \mathrm{d}E^r \int_0^\pi R(\theta^r, \theta^t) \mathrm{d}\cos\theta^t \int_0^\infty R(E^r, E^t) \mathrm{d}E^t \times \left[\sum_\beta \phi_\beta^{\text{det}} A_\beta^{\text{eff}} \right], \tag{2}$$
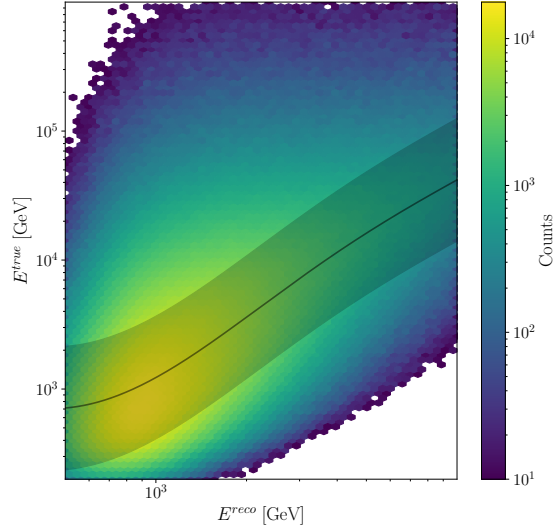
FIG. 2. Relationship between the true and reconstructed muon energy in the IceCube MC sample [4]
. Shaded area shows the 99.9th percentile limits predicted by the regressor trained on this set.

where T is the live time of the detector, and A_β^{eff} its effective area for flavor β. We use the effective area of the 86 string configuration made public by the IceCube collaboration [3]. $R(x^r, x^t)$ is a resolution function, which is responsible for the smearing between the reconstructed and true parameters x^r and x^t, respectively. We assume a log-normal distribution, giving it the form

$$R(x^r, x^t) = \frac{1}{\sqrt{2\pi}\sigma_{x^r} x^r} \exp\left[-\frac{(\log x^r - \mu(x^t))^2}{2\sigma_{x^r}^2}\right] . \tag{3}$$

As seen in Fig. 2, the energy reconstruction is biased. To model this relationship between E^{true} and E^{reco}, we train a Gaussian process regressor on the dataset [4], from which we can extract a predicted mean and standard deviation for a given E^{reco}. We then take the E^{true} points of the 99th percentile of each distribution to obtain the limits of E^{true} at which to integrate over. We have no angular resolution function since the angle resolution in Icecube for track-like events is less than 2°, making $\cos(\theta_z^{true})$ coincide with $\cos(\theta_z^{reco})$ for our study [5]. The data is from the IC86 sterile analysis [5].

B. DeepCore

In this part, we use the publically available DeepCore data sample [6] which is an updated version of what was used by the IceCube collaboration in a ν_μ disapprearance analysis [7].

The detector systematics include ice absorption and scattering, and overall, lateral, and head-on optical efficiencies of the DOMs. They are applied as correction factors using the best-fit points from the DeepCore 2019 ν_τ appearance analysis [8].

The data include 14901 track-like events and 26001 cascade-like events, both divided into eight $\log_{10} E^{reco} \in [0.75, 1.75]$ bins, and eight $\cos(\theta_z^{reco}) \in [-1, 1]$ bins. Each event has a Monte Carlo weight $w_{ijk,\beta}$, from which we can construct the event count as

$$N_{ijk} = C_{ijk} \sum_\beta w_{ijk,\beta} \phi_\beta^{\text{det}}, \tag{4}$$

where $C_{k\beta}$ is the correction factor from the detector systematic uncertainty and ϕ_β^{det} is defined as Eq. 1. We have now substituted the effect of the Gaussian smearing by treating the reconstructed and true quantities as a migration matrix.

The oscillation parameters used on our DeepCore simulations are from the best-fit in the global analysis in [9]: $\theta_{12} = 33.44°$, $\theta_{13} = 8.57°$, $\Delta m_{21}^2 = 7.42\,\text{eV}^2$, and we marginalize over Δm_{31}^2 and θ_{23}.
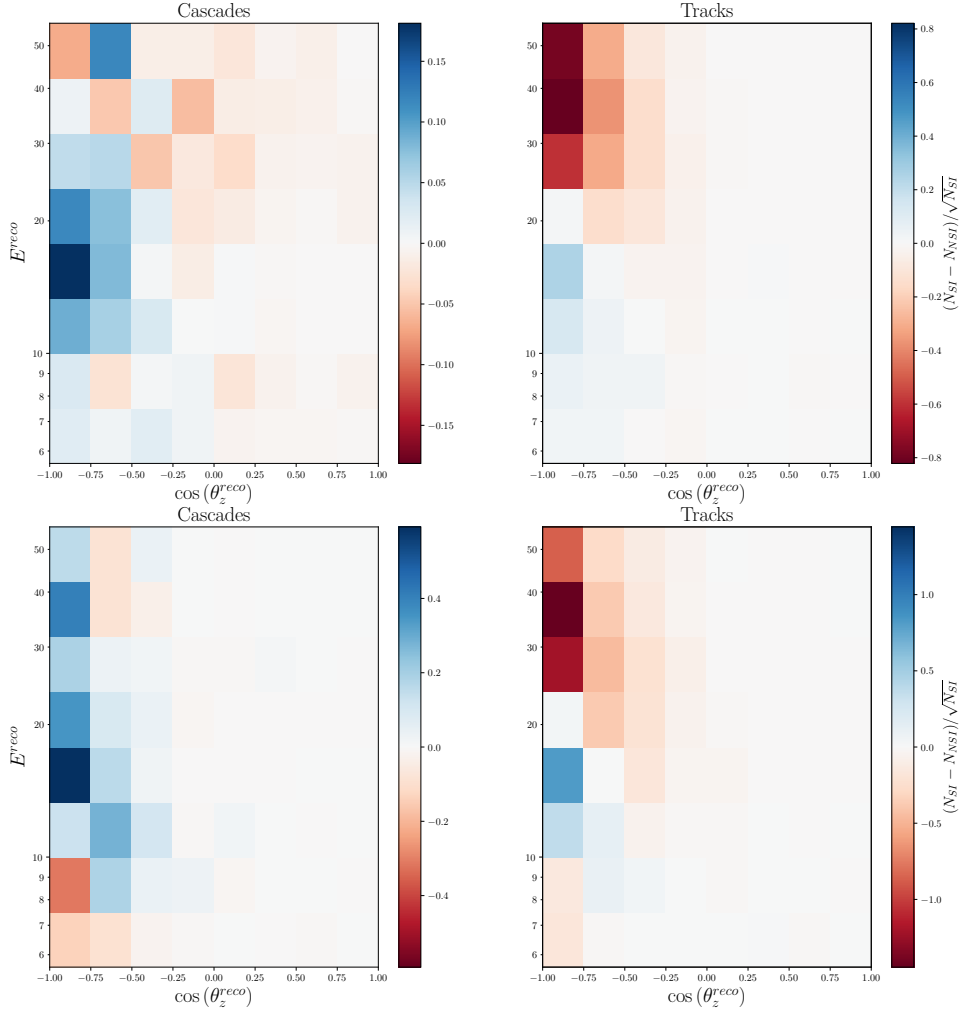
FIG. 3. Expected pulls of predicted event numbers for DeepCore and PINGU after 3 years. We compare the NSI event count with $\epsilon_{\mu\tau} = -0.05$ to the standard interaction count

We plot the event pull $(N_{NSI} - N_{SI})/\sqrt{N_{SI}}$ where $N_{(N)SI}$ are the numbers of expected events assuming (non-)standard interactions in Fig. 3. This gives the normalized difference in the number of expected events at the detector, and illustrates the expected sensitivity of DeepCore for the NSI parameters.

C. PINGU

The methodology behind the PINGU simulations are the same as with our DeepCore study I B. We use the public MC [10], which allows us to construct the event count as in Eq. 4. However, since no detector systematics is yet modelled for PINGU, the correction factors C_{ijk} are all unity. As with the DeepCore data, the PINGU MC is divided into eight $\log_{10} E^{reco} \in [0.75, 1.75]$ bins, and eight $\cos(\theta_z^{reco}) \in [-1, 1]$ bins for both track- and cascade-like events. We generate "data" by predicting the event rates at PINGU with the following best-fit parameters from [9], except for the CP-violating phase which is set to zero for simplicity.

$$\Delta m_{21}^2 = 7.42 \times 10^{-5} \, \text{eV}^2, \quad \Delta m_{31}^2 = 2.517 \times 10^{-3} \, \text{eV}^2,$$
$$\theta_{12} = 33.44°, \quad \theta_{13} = 8.57°, \quad \theta_{23} = 49.2°, \quad \delta_{\text{CP}} = 0. \tag{5}$$

II. RESULTS

For our analyses, we define our χ^2 as

$$\chi^2(\hat{\theta}, \alpha, \beta, \kappa) = \sum_{ijk} \frac{\left(N^{\text{th}} - N^{\text{data}}\right)^2_{ijk}}{\left(\sigma^{\text{data}}_{ijk}\right)^2 + \left(\sigma^{\text{syst}}_{ijk}\right)^2} + \frac{(1-\alpha)^2}{\sigma_\alpha^2} + \frac{\beta^2}{\sigma_\beta^2} \tag{6}$$

where we minimize over the model parameters $\hat{\theta} \in \{\Delta m^2_{31}, \theta_{23}, \epsilon', \epsilon_{\mu\tau}\}$, the penalty terms α and β, and the free parameter κ. N^{th}_{ijk} is the expected number of events from theory, and N^{data}_{ijk} is the observed number of events in that bin. We set $\sigma_\alpha = 0.25$ as the atmospheric flux normalization error, and $\sigma_\beta = 0.04$ as the zenith angle slope error [1]. The observed event number has an associated Poissonian uncertainty $\sigma^{\text{data}}_{ijk} = \sqrt{N^{\text{data}}_{ijk}}$.

For IceCube, the event count takes the form

$$N^{\text{th}}_{ijk} = \alpha \left[1 + \beta(0.5 + \cos{(\theta^{reco}_z)_i})\right] N_{ijk}(\hat{\theta}) , \tag{7}$$

with $N_{ijk}(\hat{\theta})$ from Eq. 2 Here, we allow the event distribution to rotate around the median zenith of -0.5.

For DeepCore and PINGU, the event count takes the form

$$N^{\text{th}}_{ijk} = \alpha \left[1 + \beta \cos{(\theta^{reco}_z)_i}\right] N_{ijk}(\hat{\theta}) + \kappa N^{\mu_{atm}}_{ijk} , \tag{8}$$

with $N_{ijk}(\hat{\theta})$ from Eq. 4. $N^{\mu_{atm}}_{ijk}$ is the muon background, which is left to float freely in the DeepCore analysis. The background at PINGU can be considered neglible to first order [10], and we thus put $\kappa = 0$ when calculating the PINGU χ^2. For IceCube, we set $\sigma^{\text{syst}}_{ijk} = f \sqrt{N^{\text{data}}_{ijk}}$. For DeepCore, we use the provided systematic error distribution which accounts for both uncertanties in the finite MC statistics and in the data-driven muon background estimate [6].

First, we set all standard oscillation parameters to their current best-fit values of Eq. 5, except for Δm^2_{31} and θ_{23}, which we marginalize over their 3σ ranges of 2.435×10^{-3} to $2.598 \times 10^{-3} \, \text{eV}^2$ and 40.1 to $51.7°$ respectively.

For the joint analysis, we follow the parameter goodness-of-fit prescription [12] and construct the joint χ^2 as

$$\chi^2_{\text{joint}} = \chi^2_{\text{IC}} + \chi^2_{\text{DC}} + \chi^2_{\text{P}} - \chi^2_{IC,min} - \chi^2_{\text{DC,min}} - \chi^2_{\text{P,min}} \tag{9}$$

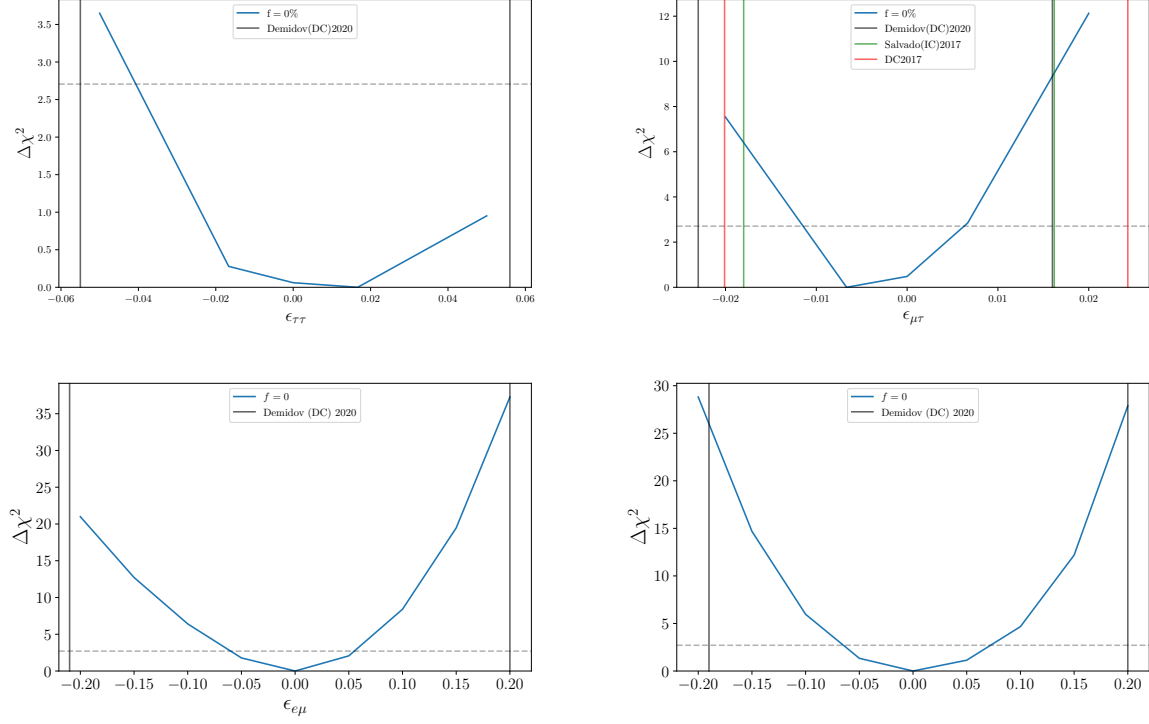with test statistic $\chi^2_{\text{joint,min}}$.

FIG. 4. The expected values of $\Delta\chi^2$ after three years of PINGU data. Δm^2_{31} and θ_{23} and have been marginalized out, and all NSI parameters not shown in each plot are set to zero.
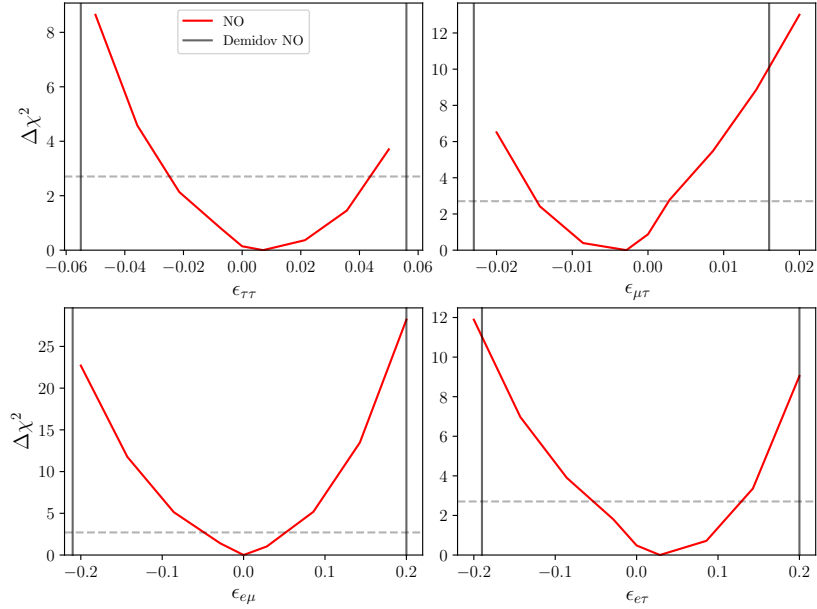

FIG. 5. The expected values of $\Delta\chi^2$ after three years of DC data. Δm^2_{31} and θ_{23} and have been marginalized out, and all other NSI parameters other than the one displayed in each panel are set to zero. The black lines show the 90% credibility region from [11]
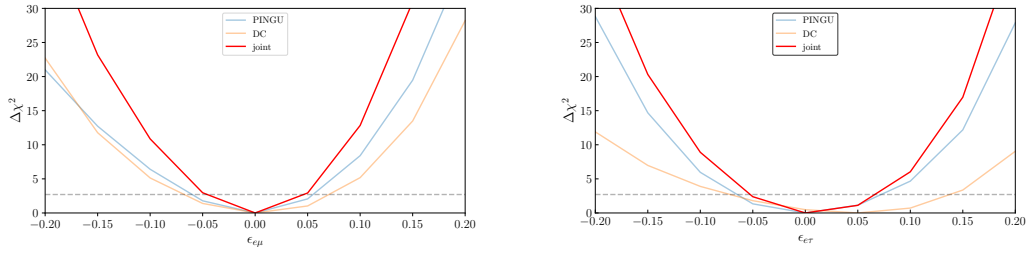
FIG. 6.

Parameter	90% CL	Best fit		
		Δm^2_{31}	θ_{23}	ϵ
$\epsilon_{\tau\tau}$	-0.028, 0.044	2.435	47.84	0.0125
$\epsilon_{\mu\tau}$	-0.015, 0.0050	2.435	43.97	-0.005
$\epsilon_{e\mu}$	-0.068, 0.070	2.435	43.97	0
$\epsilon_{e\tau}$	-0.072, 0.14	2.435	43.97	0.05

TABLE I. DeepCore results. Best fit points for Δm^2_{31} and θ_{23} are given in units of 10^{-3}eV^2 and °, respectively.

DeepCore (2017)

- ✓ Honda atmospheric fluxes
- × Only look at tracks and $\epsilon_{\mu\tau}$
- × DC Monte Carlo from an older dataset
- × 8 E bins from $6.3\,\text{eV}^2$ to $56\,\text{eV}^2$
- × 8 z bins from -1 to 0
- × Use "Overall" and "relative ν_e to ν_μ" normalization
- × Prior on spectral index
- × No zenith angle normalization
- ✓ No priors on $\Delta m^2_{31}, \theta_{23}, \theta_{13}$

Demidov (2020) DC analysis

- ✓ Honda atmospheric fluxes
- ✓ Looks at tracks + cascades for $\epsilon_{\mu\tau}$ and $\epsilon_{\tau\tau}$
- ✓ Data and Monte Carlo from DC 2018
- ✓ 8 E bins from $5.6\,\text{eV}^2$ to $56\,\text{eV}^2$
- ✓ 8 z bins from -1 to 1
- × Use "Overall" and "relative ν_e to ν_μ" normalization
- × Prior on spectral index
- × No zenith angle normalization
- ✓ No priors on $\Delta m^2_{31}, \theta_{23}$
- ✓ Fixes $\Delta m^2_{21}, \theta_{12}, \theta_{13}$
- × Uncertainty on hadron production in atmosphere
- × Uncertainty on neutrino nucleon cross section

This DC+PINGU analysis

- ✓ Honda atmospheric fluxes
- ✓ Tracks and cascades for all flavors
- ✓ Reco → true mapping from Monte Carlo migration matrix
- ✓ 8 E bins from $5.6\,\text{eV}^2$ to $56\,\text{eV}^2$
- ✓ 8 zenith angle bins from -1 to 1
- ✓ Flux normalization uncertainty of 25%
- ✓ Zenith angle uncertainty of 4%
- ✓ No priors on oscillation parameters
- ✓ Marginalize Δm^2_{31} and θ_{23}. All other oscillation parameters are fixed.

[1] M. Honda et al., Calculation of atmospheric neutrino flux using the interaction model calibrated with atmospheric muon data.`doi:10.1103/PhysRevD.75.043006`.
[2] A. M. Dziewonski and D. L. Anderson, Preliminary reference Earth model 25 (4) 297–356. `doi:10.1016/0031-9201(81)90046-7`.
[3] IceCube Collaboration, All-sky point-source IceCube data: Years 2010-2012. `doi:10.21234/B4F04V`.

Parameter	90% CL	Best fit		
		Δm^2_{31}	θ_{23}	ϵ
$\epsilon_{\tau\tau}$	-	-	-	-
$\epsilon_{\mu\tau}$	-	-	-	-
$\epsilon_{e\mu}$	-0.060, 0.055	2.517	49.2	0
$\epsilon_{e\tau}$	-0.065, 0.072	2.517	49.2	0

TABLE II. PINGU results. Best fit points for Δm^2_{31} and θ_{23} are given in units of 10^{-3}eV^2 and °, respectively.

Parameter	90% CL	Best fit		
		Δm^2_{31}	θ_{23}	ϵ
$\epsilon_{\tau\tau}$	-	-	-	-
$\epsilon_{\mu\tau}$	-	-	-	-
$\epsilon_{e\mu}$	-0.046, 0.046	2.489	47.84	0
$\epsilon_{e\tau}$	-0.057, 0.028	2.489	47.84	0

TABLE III. Joint results. Best fit points for Δm^2_{31} and θ_{23} are given in units of 10^{-3}eV^2 and °, respectively.

[4] IceCube Collaboration, Search for sterile neutrinos with one year of IceCube data.
URL https://icecube.wisc.edu/data-releases/2016/06/search-for-sterile-neutrinos-with-one-year-of-icecube-data/

[5] M. G. Aartsen et al., Searching for eV-scale sterile neutrinos with eight years of atmospheric neutrinos at the IceCube Neutrino Telescope 102 (5) 052009. doi:10.1103/PhysRevD.102.052009.

[6] IceCube Collaboration, Three-year high-statistics neutrino oscillation samples. doi:10.21234/ac23-ra43.

[7] IceCube Collaboration et al., Measurement of Atmospheric Neutrino Oscillations at 6–56 GeV with IceCube DeepCore 120 (7) 071801. doi:10.1103/PhysRevLett.120.071801.

[8] IceCube Collaboration 1 et al., Measurement of atmospheric tau neutrino appearance with IceCube DeepCore 99 (3) 032007. doi:10.1103/PhysRevD.99.032007.

[9] I. Esteban et al., The fate of hints: Updated global analysis of three-flavor neutrino oscillations 2020 (9) 178. doi: 10.1007/JHEP09(2020)178.

[10] IceCube Collaboration, IceCube Upgrade Neutrino Monte Carlo Simulation. doi:10.21234/qfz1-yh02.

[11] Bounds on non-standard interactions of neutrinos from IceCube DeepCore data - INSPIRE.
URL https://inspirehep.net/literature/1769239

[12] M. Maltoni and T. Schwetz, Testing the statistical compatibility of independent data sets 68 (3) 033020. arXiv:hep-ph/0304176, doi:10.1103/PhysRevD.68.033020.